60hp Masters Thesis
December 2016

Computational Analysis of the Thermodynamic Properties of Qubits in Open Quantum Systems using Full Counting Statistics

Alexander Davidson Bryan

Division of Mathematical Physics, Department of Physics, Lund University

Supervised by Peter Samuelsson
Co-Supervised by Fredrik Brange

LUND
UNIVERSITY

Abstract

This thesis is an attempt to understand the dynamics of qubits in the presence of a thermally interactive environment. In order to achieve this, analytically derived models were used as the basis for a computational system which simulates the evolution of qubits interacting with an environment, and calculates various thermodynamic properties of the qubits. The simulator was verified for the case of unitary evolution by comparing the results of the simulation to analytical solutions, and for more complex evolution by comparing the results to expected physical relations. The data produced by the simulator were analysed and it was found that decoherence is not unbounded with respect to energy exchange i.e. there is a specific amount of energy exchange which equates to maximal decoherence.

Contents

Acknowledgements

Thanks to Peter and Fredrik for their help in producing this thesis. Also thanks to my family for their support during my time in Lund.

Chapter 1

Introduction

Quantum information is the study of how information is encoded in quantum states, and how that information can be manipulated through the use of quantum operators. One of the most exciting potential applications of this field of study is the creation of quantum computers, which are capable of solving many problems in exponentially faster times than traditional computers [1].

For example, determining the prime factors of a number is a notoriously computationally intensive task on a traditional computer. The fastest known classical algorithm for this problem completes in sub-exponential time (as a function of the size of the input data) [2]. There is a quantum algorithm known as Shor's algorithm which takes polynomial time [3], meaning the larger the number, the faster the quantum algorithm is compared to the classical one. This has a great deal of implications for cryptography and encryption since most digital methods utilise the computational difficulty of computing the prime factors of large numbers in short times. Thankfully, quantum computation also allows for even more secure forms of cryptography [4]. It seems then that it is not only for scientific, but practical security reasons that quantum computers should be developed.

However, one of the greatest obstacles to achieving large scale quantum computers is that of decoherence, which is the decay of a quantum state into a classical one. Quantum information processing relies on quantum operators (sometimes known as quantum gates) acting as intended, with a minimal amount of error. It also requires the ability to store quantum states for a certain amount of time. Decoherence adversely affects both these properties; quantum gates will not work correctly if they act on decoherent states, and if a state is not fully isolated it will decohere, making storage of that state only possible for a limited amounts of time.

Unfortunately all physical implementations of ideal theoretical objects are imperfect and no system is ever fully isolated, so some amount of decoherence will always occur. Decoherence is particularly difficult to avoid at the scale required for accurate quantum computation.

Therefore decoherence must be well understood in order to design systems that avoid it. In this thesis we will derive an analytical model of decoherence, that makes some reasonable assumptions about the environment and how it interacts with the system. Analytical models of this type have been shown to be valid experimentally [5] and are based on widely accepted theories. This model will then be used to simulate the evolution of a qubit in an open quantum system (interacting with an environment), under the action of a time dependent Hamiltonian, and the progression of decoherence will be studied.

Chapter 2

Quantum Information

In this chapter, we will discuss the mathematical and conceptual foundations of Quantum Information. We start in Sec. 2.1 with a overview of the concepts, definitions and properties of a qubit. We then move onto a useful alternative definition of a quantum state in Sec. 2.2 and multiple qubits in Sec. 2.3

2.1 Qubits

2.1.1 Overview

The word qubit is a portmanteau of quantum and bit, bit being a word that itself is a portmanteau of binary and digit. It is the quantum analog of a bit in classical information theory. The essential difference is that unlike a bit which is in one of two definite states labeled "1" and "0", a qubit is a quantum state which is expressed in Dirac notation in as

$$|\psi\rangle = c_0 |0\rangle + c_1 |1\rangle . \tag{2.1}$$

This allows for the qubit to not only fulfil the role of a statistical ensemble of classical bits, but also to utilise phase differences between the states to create alternative ways of solving problems that would not be possible with definite states, or statistical ensembles of classical states.

A common misconception when considering the role of a qubit in quantum information and computation, is that it makes it possible to compute multiple answers to the same question at once. While it is true that a group of n qubits can be in a superposition of all possible configurations of n classical bits, making it equivalent in terms of information content to all of the separate bit configurations combined, and that a calculation performed on this state will result in a group of qubits that are in a superposition of all possible outcomes of the calculation, this information cannot be retrieved directly. This is because any measurement of the state will only yield one of the outcomes, according to the relative probabilities of the states. Instead, a faster quantum algorithm can be created by utilising the unique characteristics of quantum systems such as coherence and superposition. More explicitly, while a statistical distribution of a classical bit is a one dimensional system with a single variable describing the probability to be in either the 1 or 0 state, a qubit is multi-dimensional (as will be seen in Sec. 2.1.3) and allows for manipulations which are not possible for non quantum systems.

2.1.2 Operators

Operations performed on a qubit can be represented by unitary transformations. The reason these operations must be unitary is due to one of the most fundamental features of any quantum state, that the inner product with itself must be equal to one. From this, we can say that any transformation of the qubit should result in another qubit where the inner product with itself is also one. This can be developed mathematically to show that any transformation must be a unitary transformation.

We may also wish to describe the evolution of a qubit as a function of time. This is achieved through the use of the Schrödinger equation; a differential equation which is the fundamental quantum mechanical description of how quantum states evolve as a function of time. For this, an operator known as the Hamiltonian must be utilised, which acts as the generator of time evolution. It is also related to an infinitesimal unitary operator

$$U(dt) = I - iHdt \Rightarrow \frac{\partial}{\partial t} |\psi(t)\rangle = -iH |\psi(t)\rangle \tag{2.2}$$

which leads to the Schrödinger equation whose form arises from an axiomatic treatment of time evolution. A more detailed description of this process can be found in [6].

For cases in which the Hamiltonian is time independent, the Schrödinger equation can be easily solved and the time evolution operator takes the form

$$U(\Delta t) = e^{-i\,\Delta t\,H}. \tag{2.3}$$

It is worth noting that throughout this particular thesis, we require only analytical descriptions of time evolution in cases where the Hamiltonian is time independent. Similarly, $\hbar$ is only a scaling factor that is dependent on the units used to describe the system. In this thesis we will use Plank units in which $\hbar$ and many other fundamental constants equal one.

It is also worth noting that any Hamiltonian which acts on a qubit can be constructed through a linear combination of the Pauli Matrices. In fact these matrices play key roles throughout quantum information for many reasons, one of which will be demonstrated in the next section. It is also useful to note that, with the addition of the unit matrix, they form a standard basis for all two by two self adjoint matrices, meaning that any Hamiltonian of a two level system can be represented by a linear combination of these matrices.

2.1.3 Bloch Sphere

It can be difficult to visualise a qubit because it exists in a complex vector space which is essentially four dimensional. However, we can limit the number of dimensions needed by noting that the overall phase of any quantum state is irrelevant, as it is not physically observable and therefore we can choose the component of one of the basis vectors to be simply a real number; as long as the relative phase between the basis vectors is the same, the state will be physically identical. Additionally, a quantum state must be normalised to one which puts a restriction on the magnitude of the components of the vector, meaning they can be treated as two functions of an independent variable which when squared and then summed always returns unity. Using this knowledge we can define an alternative definition of a qubit that is easily visualisable and reveals many properties of a qubit in

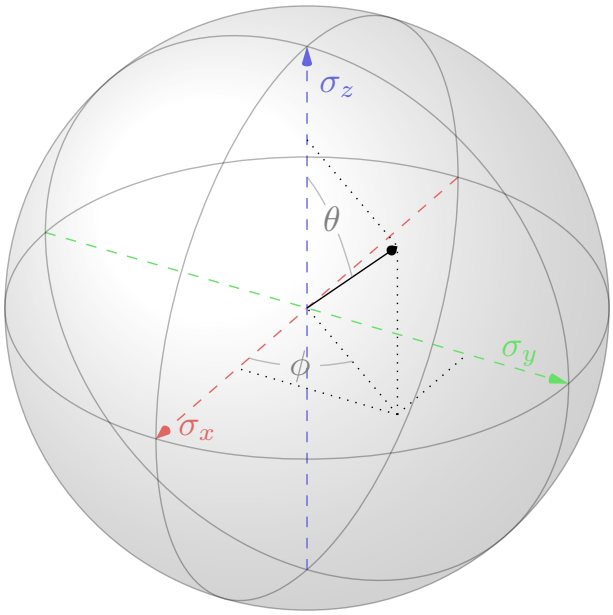

Figure 2.1: The Bloch Sphere: a representation of a quantum state as a three dimensional vector. θ and ϕ are the azimuthal and polar angles respectively. Dotted lines are shown representing the projection of the vector onto the x-y plane and onto the x and y axes

a way that is not obvious from just the numerical representation. Mathematically it is expressed as

$$|\psi\rangle = \cos(\theta/2)\,|0\rangle + \sin(\theta/2)e^{i\phi}\,|1\rangle \tag{2.4}$$

where $0 \leq \theta \leq \pi$ and $0 \leq \phi < 2\pi$. Additionally, it can be seen that as θ goes from zero to π, the state goes from being in $|0\rangle$ to $|1\rangle$, while the norm of the vector remains at unity. It can also be seen that the phase offset is directly related to ϕ. What is not obvious is that the expectation values of each of the Pauli matrices are related to these two variables such that the variables correspond to the angular components of a spherical coordinate system, where the cartesian axis of this coordinate system represents the expectations values with respect to the Pauli matrices. Moreover, the action of each of the Pauli matrices as an operator on the qubit is to rotate it around the corresponding axis by π radians. This can be seen directly by calculating the expectation values before and after the operation. This also demonstrates the strong correlation between qubits, and spin half particles. Although any two state system can represent a qubit, a spin half particle is a particularly easy way to realise a qubit, since the Pauli operators for the qubit are directly associated to the application of magnetic fields on the particle when the σ_z axis is aligned with the state corresponding to spin up.

2.2 Density Matrices

2.2.1 Definition

Density matrices are alternative definitions of quantum states that allow for classical probability distributions of quantum states. This is a fundamental notion in quantum information, as it allows a system to be described in a way which combines classical statistics with quantum mechanics, something that is essential for understanding interactions between qubits and their environment. They can also equivalently be used to describe closed quantum systems, without any reference to a classical probability. In fact this use can sometimes give a more enlightening understanding of a quantum state. A density matrix is defined as

$$\rho = \sum_n p_n \left|\psi_n\right\rangle \left\langle\psi_n\right| \tag{2.5}$$

in which p_n represents the probability for the system to be in the quantum state $|\psi_n\rangle$, implying $0 \leq p_n \leq 1$ and $\sum_n p_n = 1$.

Consider a general pure state, which is constructed using the general definition of a two level state defined in Eq. (2.4). After some algebraic manipulation we arrive at:

$$\rho = \cos(\theta/2)^2 \left|0\right\rangle \left\langle 0\right| + \frac{1}{2}\sin(\theta)(e^{-i\phi}\left|0\right\rangle \left\langle 1\right| + e^{i\phi}\left|1\right\rangle \left\langle 0\right|) + \sin(\theta/2)^2 \left|1\right\rangle \left\langle 1\right| \tag{2.6}$$

Which can be expressed more compactly in matrix form:

$$\rho = \begin{pmatrix} \cos(\theta/2)^2 & \frac{1}{2}\sin(\theta)e^{-i\phi} \\ \frac{1}{2}\sin(\theta)e^{i\phi} & \sin(\theta/2)^2 \end{pmatrix} \tag{2.7}$$

We can see that the diagonal terms describe the probability for the state to be found in either $|0\rangle$ or $|1\rangle$, as they are the squared values of the coefficients of those basis states. The off diagonal elements represent the amount of superposition between the two states, as they are non zero only for when θ is in between zero and π, with the additional factor of ϕ representing the phase difference between the two states. Note that since the state must exist in either $|0\rangle$ or $|1\rangle$, its trace must be equal to one at all times, which is satisfied in this representation.

It can be determined from the definition of the density matrix that it is self adjoint, has trace equal to one, and that it is a positive operator (see Sec 2.4 of [4]). Quantum states which can be expressed as a single outer product, are called pure states. Density matrices which cannot be expressed this way are known as mixed states. An easy way to analytically differentiate between the two types of density matrices is by calculating the purity, as given by

$$\gamma = \mathrm{Tr}\,(\rho^2). \tag{2.8}$$

The purity of a state takes of a value between one which corresponds to a pure state, and $1/n$ (where n is the dimensionality of the Hilbert space in question) which corresponds to a completely mixed state, in which, for a two state system, means the two basis states of the Hilbert space are occupied with equal probabilities.

2.2.2 Time Evolution

The time evolution of a density matrix can be determined by considering the evolution of the component quantum states. Since the evolution of each state is described by a

unitary operator, we need only insert this operator into the correct places whilst noting that the unitary operator must be conjugated before acting on the bra [6]. Hence the time evolution of a density matrix through a system described by a unitary matrix U can be formulated by

$$\rho(t) = \sum_n p_n U \left|\psi_n(t_0)\right\rangle \left\langle\psi_n(t_0)\right| U^\dagger = U\rho(t_0)U^\dagger. \tag{2.9}$$

This can be expressed as a differential equation called the Liouville-Von Neumann equation by using a reformulation of the Schrödinger equation in terms of the time evolution operator rather than the state, and is expressed as

$$\frac{\partial}{\partial t}\rho(t) = -i[H(t), \rho(t)]. \tag{2.10}$$

A more explicit derivation can be found in section 3.1.1 of [7].

2.2.3 Expectation Values

One might ask why we use the density matrix at all, and why we don't just use superposition? It could naively be assumed that if a combination of two quantum states was desired in such a way that it represented a probability distribution of those states, then only a superposition of those states would be necessary: Although this would be valid for measurements of those exact states, there are other properties which would not correspond to our desired concept of a classical distribution of quantum states. In particular the expectation value of such a state contains terms which would not exist for a classical distribution.

Instead, we define another operation as the expectation value for a density matrix, the trace of an operator acting on the density matrix. We can demonstrate the action of this operation on a two level system as follows;

$$\begin{aligned} A\rho &= pA\left|\psi\right\rangle\left\langle\psi\right| + (1-p)A\left|\phi\right\rangle\left\langle\phi\right| \\ \mathrm{Tr}(A\rho) &= p\left\langle\chi_1\right| A\left|\psi\right\rangle\left\langle\psi|\chi_1\right\rangle + (1-p)\left\langle\chi_2\right| A\left|\phi\right\rangle\left\langle\phi|\chi_2\right\rangle \\ &= p\left\langle\psi|\chi_1\right\rangle\left\langle\chi_1\right| A\left|\psi\right\rangle + (1-p)\left\langle\phi|\chi_2\right\rangle\left\langle\chi_2\right| A\left|\phi\right\rangle \\ &= p\left\langle\psi\right| A\left|\psi\right\rangle + (1-p)\left\langle\phi\right| A\left|\phi\right\rangle. \end{aligned} \tag{2.11}$$

As we can see, this form produces the desired result, where the expectation value of the each of the pure states is found, with a probability equivalent to being in that state.[1]

2.3 Concurrent Systems and the Tensor Product

2.3.1 Definition

For systems which involve multiple qubits, we can construct a basis for the Hilbert space which encompasses all the possible states of the system. This is done through the use of the tensor product, which is a binary vector operation, taking two tensors and producing a single tensor. The tensor product is a one to one mapping, with each configuration of

[1] $|\chi_i\rangle$ represent an arbitrary basis, aditionally the identity $\sum_i |\chi_i\rangle\langle\chi_i| = I$ is used. For more information about the trace see [4]

the two input tensors having a unique tensor representation. More information can be found in chapter 1.2.1 of [4]. The Hilbert space of two concurrent systems can be written as the tensor product of their Hamiltonians,

$$H_A \otimes H_B \tag{2.12}$$

and the basis states as all the possible tensor products of the basis states of the systems. For example if the two concurrent systems are qubits, the basis states will be:

$$|0\rangle \otimes |0\rangle\,,\ |0\rangle \otimes |1\rangle\,,\ |1\rangle \otimes |0\rangle\,,\ |1\rangle \otimes |1\rangle\,. \tag{2.13}$$

Since a qubit has a Hilbert space with dimension 2, n qubits together will have a Hilbert space of dimension 2^n as there will be 2^n possible combinations of n two state systems. Similarly the density matrix of concurrent systems can also be expressed as the tensor product of the individual density matrices comprising the component systems.

2.3.2 Seperability and the Reduced Density Matrix

If a state can be written as

$$\rho = \sum_k p_k \rho_k^A \otimes \rho_k^B \tag{2.14}$$

then it is a separable state, and if not, it is entangled. This can also be said of pure states, more information can be found in [4]. A density matrix for subsystems of a larger system can be found using the reduced density matrix. If the state of the larger system is not a separable state, then even if the density matrix of the whole system is pure, its reduced density matrices (the density matrices of the subsystems) will not be. The reduced density matrices for a system are defined using the partial trace, which is similar to the trace but only over the basis of the one of the component systems. For example the reduced density matrix of one of the qubits in a two qubit system is defined as

$$\rho_A = \langle 0|_B \rho_{AB} |0\rangle_B + \langle 1|_B \rho_{AB} |1\rangle_B\,. \tag{2.15}$$

This can be extended for larger systems thusly

$$\rho_A = \sum_k \langle k| \rho_{AB} |k\rangle \tag{2.16}$$

where $|k\rangle$ represents a basis of system B.

Chapter 3

Open Quantum Systems

3.1 Classical Noise

We begin the discussion of how random fluctuations can affect the state of a system by considering first a classical bit. A random fluctuation in this case is a probability p for the bit to flip its values, meaning that the probability for the system to be unaffected will be $p-1$. This can be expressed as a matrix equation with the vectors representing the probability to be in either of the two classical states,

$$\begin{pmatrix} p-1 & p \\ p & p-1 \end{pmatrix} \begin{pmatrix} p_0 \\ p_1 \end{pmatrix} = \begin{pmatrix} (p-1)\,p_0 + p\,p_1 \\ p\,p_0 + (p-1)\,p_1 \end{pmatrix}. \tag{3.1}$$

We can see that the fluctuations only depend p and the populations of the initial state. We can also consider combining this noise operator with an action we wish to perform on the bit. For example if we wish to flip the bit, but assume that the process is only successful with probability p, then we only need to swap the columns of the operator in Eq. (3.1). If we were then to apply further similar operators on the bit, and assume that the probabilities for their success are independent on the previous operator applied to them, then the system would be described as a Markovian. This is an important property as it greatly simplifies the system that needs to be determined. All of this can be extended to the quantum case.

3.2 Kraus Operators

If we wish to create operators similar to those in Eq. (3.1) but for a quantum system, we require the system to be open, meaning the system we are concerned with is interacting with some external system. This is necessary since an operator in a closed (i.e. non interacting) system is required to be unitary. Therefore to model a system described by a density matrix ρ_S undergoing random fluctuations, we require a definition of a larger system

$$\rho = \rho_S \otimes \rho_E \tag{3.2}$$

where ρ_E represents an external system that we will call the environment. In writing this we assume that the system and environment are in a product state, an assumption that is usually true since when a quantum system is initially produced it should be independent from its enviroment. This combined system can then be subjected to some unitary transformation

$$U\rho\,U^\dagger = U(\rho_S \otimes \rho_E)\,U^\dagger. \tag{3.3}$$

Note that the combined system is now no longer necessarily separable as the unitary transformation can mix terms between ρ_S and ρ_E. Detailed knowledge of the environment, enough to define a density matrix, is in most physical cases nearly impossible to find. Hence we will find the reduced density matrix corresponding to the system after the evolution, by taking the partial trace

$$\rho'_S = \sum_k \langle k| U(\rho_S \otimes \rho_E) U^\dagger |k\rangle \tag{3.4}$$

where $|k\rangle$ are the basis states of the environment. As mentioned previously, the parameters of the environment are nearly impossible to obtain. As such the basis states will not be known. However we can simplify this system by assuming the environment initially starts in some pure state $|E\rangle$. This assumption does not reduce the generality of the formulation, since if the environment is not in a pure state, we can dictate that there must exist some auxiliary system which is in a pure state[1]. This leads to an alternative definition of ρ'_S

$$\rho'_S = \sum_k \langle k| U(\rho_S \otimes |E\rangle \langle E|) U^\dagger |k\rangle = \sum_k E_k \rho_S E_k^\dagger \tag{3.5}$$

where $E_k = \langle k| U |E\rangle$ is known as a Kraus operator. We also find that

$$\begin{aligned} \sum_k E_k^\dagger E_k &= \sum_k \langle E| U^\dagger |k\rangle \langle k| U |E\rangle \\ &= \langle E| U^\dagger U |E\rangle = I \end{aligned} \tag{3.6}$$

since the $|k\rangle$ states form an orthogonal basis. This basis set is arbitrary and the choice of the basis will change the E_k operators, but still represent the same interaction between the environment and the system. The relation between these representations of E_k is a simple unitary transformation similar to any other change of basis.

The Kraus operators allow us to define the evolution of a system interacting with an environment, without having to determine the exact state of the enviroment. Moreover, the Kraus operators can be defined without deriving them as we have done here. As long as they fulfil the condition stated in Eq. 3.6 they will be valid operators for modelling the evolution of an open quantum system. Examples of Krauss operators can be found in Chapter 8 of [4], but here we only need note that any operator fulfilling the condition stated in Eq. 3.6 can model the quantum analogue of the kind of operation described in Sec. 3.1.

3.3 Master Equations and the Lindblad Equation

Although we now have a way to describe the evolution of a system in contact with an environment whose exact characteristics are unknown, we can only work with one action at a time. For example if we wished to know how the system evolved over two different lengths of time, we would need two different Kraus Operators. What we define in this section describes a continuous interaction and follows the method described in Sec. 8.4.2 of [8].

[1]This eventually leads to the conclusion that the quantum state of the universe must be a pure state, since the universe is the largest possible system which any other system must be a subsystem of.

However, this description will only be valid if the system is Markovian as described is Sec. 3.1. What this means in terms of continuous motion is that the action of the environment has only first order dependence of time. We can physically interpret this as saying that the environment has no "memory" of what it has done to the system before and its action at each instance of time is independent of all other states. This a reasonable assumption to make when the environment is much larger and more complex than the system it is interacting with, since if the state of the system did have an effect on the state of the environment it would most likely be overpowered by the environments own internal variation.

If we consider the non-unitary evolution of a system from t to $t + dt$ we can describe this in Kraus operator representation as

$$\rho(t + dt) = \sum_k E_k(dt)\rho(t)E_k(dt)^\dagger \tag{3.7}$$

With the Krauss operators defined as a function of time. If we then take the limit $dt \to 0$ we can expand the Kraus operators as

$$E_k = E_k^{(0)} + \sqrt{dt}E_k^{(1)} + dtE_k^{(2)} + \mathcal{O}(dt\sqrt{dt}). \tag{3.8}$$

Since the Kraus operators are determined by an arbitrary choice of basis, we can choose a basis such that the first element in the expansion is

$$E_0 = I + dt(M - iH) + \mathcal{O}(dt^2) \tag{3.9}$$

with arbitrary hermitian operators[2] M and H. In order for the system to be Markovian, we require that $\rho(t+dt) = \rho(t) + d\rho dt$. In other words it must be a first order derivative, since higher orders require knowledge of the interaction between the environment and previous states. In order to fulfil this requirement, the other Kraus operators in the basis set must be

$$E_k = \sqrt{dt}L_k + \mathcal{O}(dt) \text{ for } k > 0 \tag{3.10}$$

and all orders of dt higher than dt^2 for E_0 and dt for $E_{k>0}$ must be ignored, as can be seen when these definitions are inserted into Eq. 3.7

$$\begin{aligned}\rho(t + dt) &= E_0\rho(t)E_0^\dagger + \sum_{k>0} E_k\rho(t)E_k^\dagger \\ &= (I + dt(M - iH))\rho(t)(I + dt(M + iH)) + dt\sum_k L_k\rho(t)L_k^\dagger \\ &= \rho(t) - idt[H, \rho(t)] + dt\{M, \rho\} + dt\sum_k L_k\rho(t)L_k^\dagger\end{aligned} \tag{3.11}$$

M can be solved for in terms of L_k since the Kraus Operators must satisfy the normalisation condition outlined in Eq. (3.6)

$$\begin{aligned}\sum_k E_kE_k^\dagger = I &= (I + dt(M - iH))(I + dt(M + iH)) + dt\sum_k L_kL_k^\dagger \\ &= I + 2dtM + dt\sum_k L_kL_k^\dagger \\ \Rightarrow M &= -\frac{1}{2}\sum_k L_kL_k^\dagger\end{aligned} \tag{3.12}$$

[2]We will see later that H can be equated with the hamiltonian of the system without the effect of the enviroment

Which leads to

$$\rho(t+dt) = \rho(t) - idt[H,\rho(t)] + dt\sum_k \left(L_k\rho(t)L_k^\dagger - \frac{1}{2}\{L_kL_k^\dagger,\rho\}\right)$$
$$\Rightarrow \frac{\rho(t+dt)-\rho(t)}{dt} = \frac{\partial\rho(t)}{\partial t} = -i[H,\rho(t)] + \sum_k \left(L_k\rho(t)L_k^\dagger - \frac{1}{2}\{L_kL_k^\dagger,\rho(t)\}\right) \tag{3.13}$$

which is the Lindblad master equation.

Its form is very similar to that of the Liouville-von Neumann equation, but with an additional part, which describes the dissipation of the system. We can also now equate the H operator with the Hamiltonian of the system, if it were not interacting with the environment. There are very many possible L_k operators, which are known as Lindblad operators, which represent different types of interaction with the bath. They are operators in the Hilbert space of the system, since they are derived from the Kraus operators which are also in the systems Hilbert space. A set of Lindblad operators that will be particularly important in this thesis are those representing a fluctuation between the different eigenstates of a system, when it interacts with a thermal bath. The Lindblad operators for this interaction are

$$\begin{aligned} L_-^{i,j} &= \sqrt{\Gamma_-}S_{i,j} \\ L_+^{i,j} &= \sqrt{e^{-\beta\nu}\Gamma_-}S_{i,j}^\dagger \end{aligned} \tag{3.14}$$

Where $S_{i,j} = |i\rangle\langle j|$ is a kind of ladder operator corresponding to moving from eigenvector $|j\rangle$ to $|i\rangle$ and eliminating all other eigenvectors. ν is the difference between the eigenvalues of the two states and β is the temperature of the environment where the environment is assumed to be a heat reservoir where changes in energy of the system do not effect the temperature of the enviroment. Γ_- is the rate at which the state will spontaneously go from $|j\rangle$ to $|i\rangle$, akin to the probability p in 3.1. The coefficient of $S_{i,j}^\dagger$ is determined as a function of Γ_- though the use of detailed balance relations, which ensure that the system will tend to a thermal equilibrium with its environment. More information about this formulation can be found in [8].

3.4 Quantum Thermodynamics

There are many ways in which statistical mechanics and quantum mechanics can be combined and in this section we will cover some quantum extensions of classical thermodynamic notions. This will enable the study of various phenomena of open quantum systems in a way that is more intuitive than simply looking at expectation values. However, all quantum theories that take thermodynamics into account are still completely valid quantum theories, with no additional assumptions having to be made about the systems involved other than the standard axioms of quantum mechanics. Additionally there is a uniquely quantum thermodynamic analysis that can be carried out using the process of full counting statistics, which will be discussed in Sec 3.4.3.

3.4.1 Relation to Classical Thermodynamics

Quantum Extension of the First Law of Thermodynamics

One of the fundamental parts of classical thermodynamics is the first law, which states that in a body which does not exchange mass with its enviroment, the change in the internal energy is equal to the amount of work done on the system by its environment plus the amount of heat exchanged from the environment to the system. This can be expressed mathematically as

$$\Delta U = \Delta Q + \Delta W. \tag{3.15}$$

We can form a quantum version of the same law, but instead stating that the equality holds for the averages of these values. This is not really so far from the classical version, since these values are in actuality, statistical averages over the kinetic energy of the constituent molecules of the system. If we define the average internal energy of the system as the expectation of the hamiltonian, we can derive a form of the first law in the infinitesimal case by simply considering the derivative

$$\frac{\partial}{\partial t}\operatorname{Tr}(H\rho) = \operatorname{Tr}\left(\frac{\partial H}{\partial t}\rho\right) + \operatorname{Tr}\left(H\frac{\partial \rho}{\partial t}\right) \tag{3.16}$$

Since $\partial \operatorname{Tr}(H\rho)/\partial t$ is the change in average energy of the system, we can consider the other two parts, derived from the partial derivative, to be equivalent to work and heat. Since the first term in the sum is the change in the energy of the system due to its Hamiltonian, we can consider this work done on the system, described by its Hamiltonian. The other term can be considered almost as the expectation value of energy for the change in the state. Since under unitary evolution this value is always zero (see Sec. A.1.1) we can equate it with some amount of energy exchange with the environment, without the action of the Hamiltonian, and as such we identify this as heat. A more detailed examination of this formula can be found in[9]. This equation is used in almost all quantum thermodynamics and is well established.

Gibbs state

A fundamental notion in thermodynamics is the equilibrium state of a system with its environment. This is determined by finding the state of maximum entropy, or equivalently the state which is invariant under time evolution of the system. This is also known as the canonical ensemble of a system. For classical systems this can be determined by

$$P_i = \frac{\exp(-\beta E_i)}{Z} \tag{3.17}$$

where P_i is the probability to be in state i, β is the inverse temperature which is defined as[3] $1/T$ and E_i is the energy of that state. Z is the partition function, which normalises the probabilities so their sum is one, which is defined as

$$Z = \sum_i \exp(-\beta E_i). \tag{3.18}$$

Both these equations are derived in [10].

[3]The definition in SI is $1/(k_B T)$

The quantum extension of this notion is

$$\rho = \frac{\exp(-\beta H)}{\mathrm{Tr}\left(\exp(-\beta H)\right)} \tag{3.19}$$

which produces the same results as the classical version when attempting to compute the probability to be in a particular eigenstate of the hamiltonian. The justification for this representation is that it is necessary in order for the state to have the same probability distribution for the energies of the system as described in the classical Gibbs state.

3.4.2 Fluctuation Theorems

There have been more recent developments which come from modern statistical mechanics, relating the probability for a certain transition between states, the probability for the time reversed version of the same transition and the work done on the system, as well as the change in the free energy of the system. It is derived in [11] and defined as

$$\frac{P_{fwd}^{i\to j}}{P_{rev}^{j\to i}} = \exp(\beta(W_{i\to j}) - \Delta F) \tag{3.20}$$

where; $P_{fwd}^{i\to j}$ is the probability to go from state i to state j in the forward time regime, $P_{rev}^{j\to i}$ is the probability to go from state j to state i in the reverse time regime, $W_{i\to j}$ is the work done on the system as it goes from i to j, and ΔF is the free energy difference between the two states. This equality can be used to check the accuracy of the work exchange distributions that will be calculated using Full Counting Statistics.

3.4.3 Full Counting Statistics

Given a description of an open system based on the density matrix, it is not immediately apparent what the probability distribution for exchanges in work and heat are. However there is a method which allows for calculation of these probabilities, as outlined in [12]. This method is called full counting statistics, and uses the addition of a counting field, to keep track of the work and heat exchanges with the system, using the two point measurement description of work an heat transfer, a description of which can be found in [13]. These counting fields are added into parts of the Lindblad operators described in Eq. (3.3), which leads to this form of the Lindblad equation:

$$\begin{aligned}\dot{\rho}(t,u) = -i[H,\rho(t)] + \sum_k \Gamma_- e^{\nu_k} \\ \left(e^{iu} S_k \rho(t) S_k^\dagger - \frac{1}{2}\{S_k^\dagger S_k, \rho(t)\} + e^{-(\beta+iu)} S_k^\dagger \rho(t) S_k - \frac{1}{2} e^{-\beta}\{S_k S_k^\dagger, \rho(t)\}\right).\end{aligned} \tag{3.21}$$

This results in the state being a function of two independent parameters, although it should be noted that the states corresponding to $u \neq 0$ are unphysical and merely part of the mathematical apparatus used in full counting statistics. From this state it is possible to obtain the Fourier transform of the probability distributions of both work and heat. We call the Fourier transform of a probability distribution the characteristic function and of course the inverse Fourier transform can be taken to retrieve the probability distribution. Additionally, the moments (average, variance, skewness, etc.) of the distribution can be calculated by

$$\mathrm{E}(X^n) = i^n \phi_X^{(n)}(0) \tag{3.22}$$

where $\mathrm{E}(X^n)$ is the nth moment of variable X and $\phi_X^{(n)}(0)$ is the nth derivative of the characteristic function of X evaluated at zero. The characteristic functions can be calculated from the state $\rho(t,u)$ as

$$\phi_W(u,t) = \mathrm{Tr}(e^{iuH(t)}\rho_w(t,u)) \tag{3.23}$$

$$\phi_Q(u,t) = \mathrm{Tr}(\rho(t,u)) \tag{3.24}$$

where ϕ_W is the work characteristic function and ϕ_Q the heat characteristic function. Also, when calculating the work distribution, the initial state of the system must be modified in the following way

$$\rho_w(0,u) = e^{-iuH(0)}\rho(0). \tag{3.25}$$

Chapter 4

Methods

In this section we will discuss the methods used to simulate the various systems described in the analysis. The final version of the simulator uses C++ to generate the states and perform the full counting statistics. Mathematica is used to plot and analyse the data. The output from the C++ program is: a list of all density matrices calculated where increasing position in the list represents time; an array of probability values where one dimension equates to time and the other to change in work/heat and a similar array but where the list elements are the values of the characteristic function. Additionally the Hamiltonian for each time step calculated is output in a list, and all the previous datasets are also output for the time reversed evolution.

4.1 Basic Method

Many iterations of the software were written over the course of this project, but they all have the same fundamental principle; that any time evolution of an open or closed quantum system can be approximated by applying many time invariant operators corresponding to small time differences in a sequence that respects time ordering. The accuracy of this method depends on the size of the time steps being used. Although in principle arbitrarily sized time steps could be used, equally sized time steps were chosen for ease of use. The accuracy of the simulation will be dependent on the resolution of these time steps, and whether they can accurately encapsulate the time dependence of the system in question.

The simplest example of this is when approximating closed evolution due to an arbitrary Hamiltonian of a state vector. The approximate time evolution can be described via an iterative algorithm with N steps, stated in Eq. (4.2), which computes each next state using a time evolution operator. For example if the time evolution of the state is governed by a differential equation of a single left acting operator O, then the time evolution operator will be

$$\begin{aligned} T(t_n) &= e^{-i\,\Delta t\, O(t_n+\Delta t/2)} \\ |\psi(t_n+\Delta t)\rangle &= T(t_n)\,|\psi(t_n)\rangle \\ \rho(t_n+\Delta t) &= T(t_n)\rho(t_n)U^\dagger. \end{aligned} \tag{4.1}$$

$$N\begin{cases} |\psi(\Delta t)\rangle & = T(0)\,|\psi(0)\rangle \\ |\psi(2\Delta t)\rangle & = T(\Delta t)\,|\psi(\Delta t)\rangle \\ & \vdots \\ |\psi(t_f-\Delta t)\rangle & = T(t_f-2\Delta t)\,|\psi(t_f-2\Delta t)\rangle \\ |\psi(t_f)\rangle & = T(t_f-\Delta t)\,|\psi(t_f-\Delta t)\rangle \end{cases} \tag{4.2}$$

The accuracy of this method depends greatly on the size of the time steps but also on the length of time the simulation represents. If the ratio of these two parameters is not sufficient enough to capture the features of the Hamiltonian (something akin to the Nyquist frequency), the simulation will not be accurate. Additionally, small errors will become more significant over time, as the method for calculating the next state uses the previously calculated state, which amplifies the error in the calculation of the previous state.

4.2 Additional Techniques

This section describes the methods used in the simulation to calculate various parameters. Most of these techniques do not add any physical interpretation to the model, and just describe the numerical and mathematical methods used in the simulation.

4.2.1 Lindblad Superoperator and Vectorisation

To use the method exactly as described in Sec. 4.1 we require an equation which is only a differential equation of a single left acting operator, the lindblad equation does not satisfy this criterion. However, it can be converted into its superoperator form, which is most easily achieved by converting the density matrix in question into a vector, and applying a linear transformation to it which is equivalent to the action of the Lindblad equation. The process can be achieved using these methods:[14]

$$\rho = \begin{pmatrix} \rho_{11} & \rho_{12} & \cdots \\ \rho_{21} & \rho_{22} & \cdots \\ \vdots & \vdots & \ddots \end{pmatrix} \rightarrow \begin{pmatrix} \rho_{11} \\ \rho_{21} \\ \vdots \\ \rho_{12} \\ \rho_{22} \\ \vdots \end{pmatrix} = \vec{\rho} \tag{4.3}$$

$$A\,\rho\,B \rightarrow (B^T \otimes A)\,\vec{\rho}. \tag{4.4}$$

4.2.2 Discrete Differentiation

To calculate the work and heat change in a system as described in Sec. 3.4.1, the derivative of both the Hamiltonian and state is required. The derivative of the Hamiltonian in most cases can be determined analytically, either by hand or with symbolic programming. For the state, the derivative can be estimated by using the limit form of the derivative for any given order, and explicitly calculating it for a small separation, rather than for the limit.

4.2.3 Full Counting

In order to calculate the full counting statistics, a range of values for the characteristic function must be sampled over which the function is periodic. Additionally, much like the sampling of the states/Hamiltonian we require a small enough resolution of steps in the characteristic parameter is required so that the system is accurately represented when discretised. The software then simulates the same time evolution for each value of the characteristic parameter and saves this as a subarray in a larger array of states. During this time evolution the level spacing (separation between energy eigenvalues) must be calculated along with the lowering/raising operator which is the outer product of two eigenvectors, $|E-\rangle \langle E+|$ for lowering and the hermitian of this operator for the raising operator. This is then used in the Lindblad superoperator. The characteristic function is then calculated from each of these arrays of states, to give another set of arrays which is a discretisation of the characteristic function as a function of time and the characteristic parameter. These arrays are then inversely Fourier transformed in order to retrieve the probability distributions for each time step. The index of the distribution is related to the amount of energy exchange by the level spacing.

4.2.4 Time Reversal

In order to determine the validity of the Crooks Fluctuation Theorem a reverse time evolution must be performed. This is done via a similar process as described in Sec. 4.1 but with the order of iteration reversed, and using time reversed Liouville-von Neumann part of the Lindblad equation, which is equivalent to taking its complex conjugate. Since the Lindblad Operators are time invariant, they are calculated in the same way as the forward time evolution.

4.3 Simulation Validity

In order to test the validity of the simulation, the evolution of a qubit under a unitary transformation with no effect from the environment was calculated. In the simulation this is done by changing the loss rate to zero, reducing the Lindblad equation to the Liouville-von Neumann equation. Since through much of this analysis a Rabi cycle type Hamiltonian will be used, it is essential the the simulation reproduce the expected behaviour in the unitary case. Fig. 4.1 shows the difference between the main attributes of the computed state and an analytically derived result (calculated symbolically in Mathematica see B.1.2 for details).

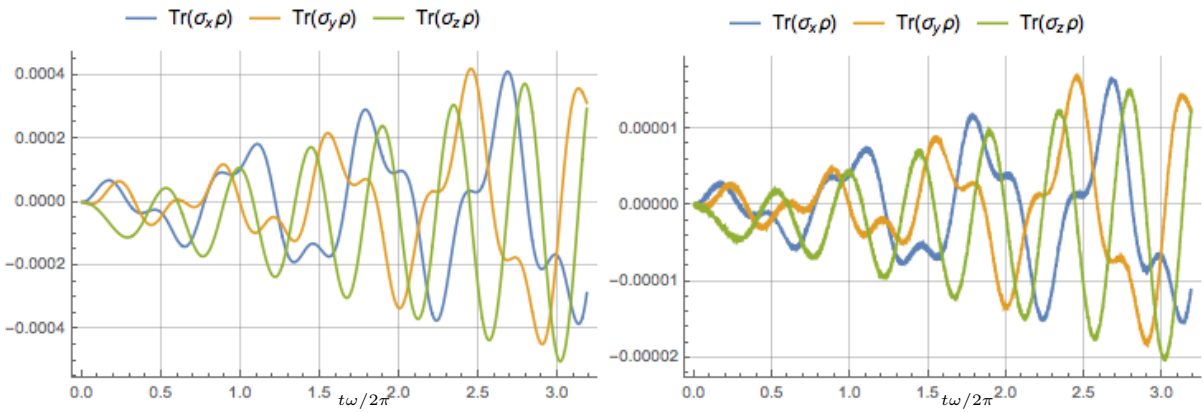

(a) (b)

Figure 4.1: Difference between computed and analytical state attributes with Hamiltonian $\cos(t)\,\sigma_x + \sin(t)\,\sigma_y$, initial state $|1\rangle$, time range $= 6\pi$ and (a) 1000 (b) 5000 time steps. X-axis shows the simulated time, normalised by an arbitrary frequency ω.

The difference between the computed and analytic result is quite small, although the error does grow over the course of the simulation as was discussed in Sec. 4.1. The Hamiltonian used here is not one that will be used in this analysis, it used just to test the validity of the simulator. The types of Hamiltonians that will be used in the actual analysis are those with constant eigenvalues. As such the Hamiltonian shown in Fig. 4.2 is much more representative of the type of Hamiltonian that will be simulated. When interactions with the environment are added to the simulation, a steady state is usually reached around the end of the time span represented here, after this point the errors should minimise since the state becomes static. However even in the unitary case shown here, the error is within reasonable margins. If it becomes necessary to increase the accuracy for a particular simulation, the time steps can be increased accordingly, which will increase the accuracy of the simulation. This can be repeated until no significant change occurs between the time step increases.

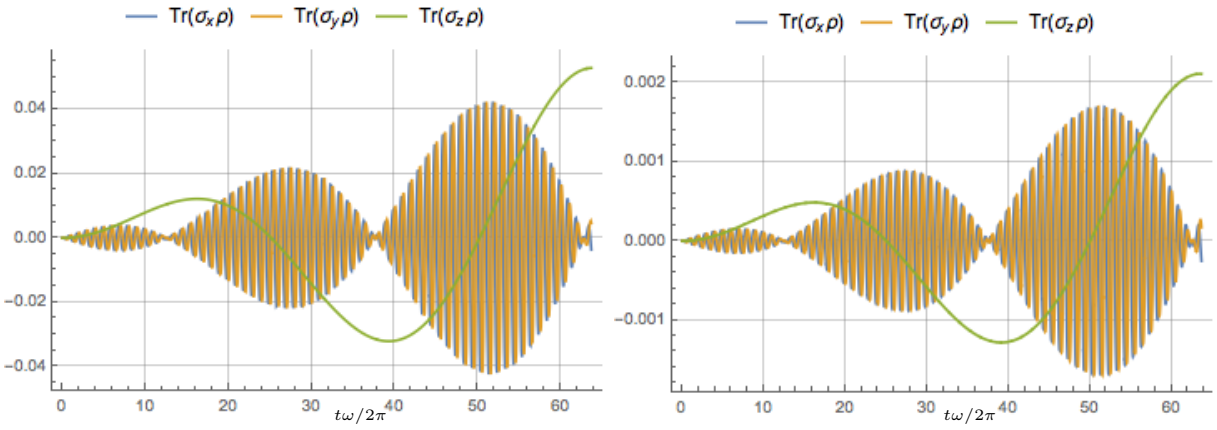

(a) (b)

Figure 4.2: Difference between computed and analytical state attributes with Hamiltonian $0.5\,I + 0.01\,\cos(t)\,\sigma_x + 0.01\,\sin(t)\,\sigma_y + 0.5\,\sigma_z$, initial state $|1\rangle$ for (a) 1000 (b) 5000 time steps.

An analytic solution to the Lindblad equation for a time dependent Hamiltonian is more difficult to obtain than for unitary evolution, as such validity of this simulation will be based predominantly upon the Crooks Fluctuation Theorem, as shown in Sec. 4.3.1. Additionally some physical intuition about the expected motion of the qubit can be applied in order to determine the validity of the simulation, if not the precision of the numerics. Furthermore different methods of computing the same physical parameters can be compared, and the extent to which they match can also determine the accuracy of the simulation, which is also shown in Sec. 4.3.1.

4.3.1 Full Counting Statistics Validity

Full counting statistics is also used in the following simulations. As such, methods to test the validity of these calculations is required, however analytic solutions are become increasingly difficult (if they were not, there would not be much reason for simulating them). However two approaches can be utilised by testing whether the simulations fulfil certain theorems. One is the First Law of Thermodynamics, expressed in its quantum form as shown in Sec. 3.4.1. The other is the Crooks Fluctuation Theorem, which is shown in Sec. 3.4.2.

In order to test whether the simulation fulfils the First Law, we can calculate the averages of work and heat using only the computed states, and comparing this to the first moment of the characteristic function as described in Sec. 3.4.3.

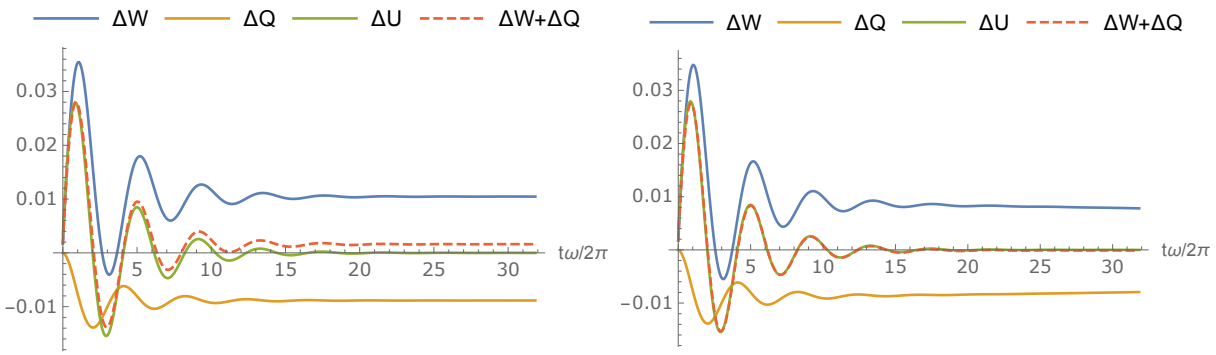

Figure 4.3: (a) shows the calculated values for the change in work ΔW, heat ΔQ, energy ΔU and the sum of the computed values of work and heat when using the direct method of calculation. (b) shows the same values but when using the characteristic function computed by using full counting statistics. The hamiltonian used is given in the appendix (Sec. B.1). The system was simulated with a loss rate of 0.02 and an inverse temperature of 2

Fig. 4.3 shows the same physical parameters for the two methods of calculation, and shows how they match each other in both magnitude and time dependence. The first law tells us that the sum of the average work and heat should be equal to the expectation value for the energy. This is verified for both methods of calculation, however using the characteristic function gives slightly more accurate results. This is likely due to the fact that the characteristic function is changing less as a function of its argument, than the states are changing in time. This means that the discrete approximation of derivative of the characteristic function is more accurate than that of the states.

The Crooks fluctuation theorem was also tested for the same system, as shown in Fig. 4.4. This test does not always give reliable data as many of the computed probabilities for exchanges in work and heat are close to zero. When these values are close to zero floating point errors play a larger part and as such the ratio of any two such numbers becomes randomly distributed and does not exhibit the expected behaviour. However, the system can be chosen such that large probabilities are found for both probabilities (as will be discussed in the analysis) and it was such a system that was chosen here. As can be seen, the relation holds for work exchanges far from zero. One part of the theorem that was unable to be fully explored is the dependence on the change in free energy. As the eigenvalues of the system must be kept constant (in order to calculate the full counting statistics) there can be no change in free energy. Regardless the CFT test shows that the simulation is physically valid for all situations the will be explored here, as far as fluctuation theorems are concerned.

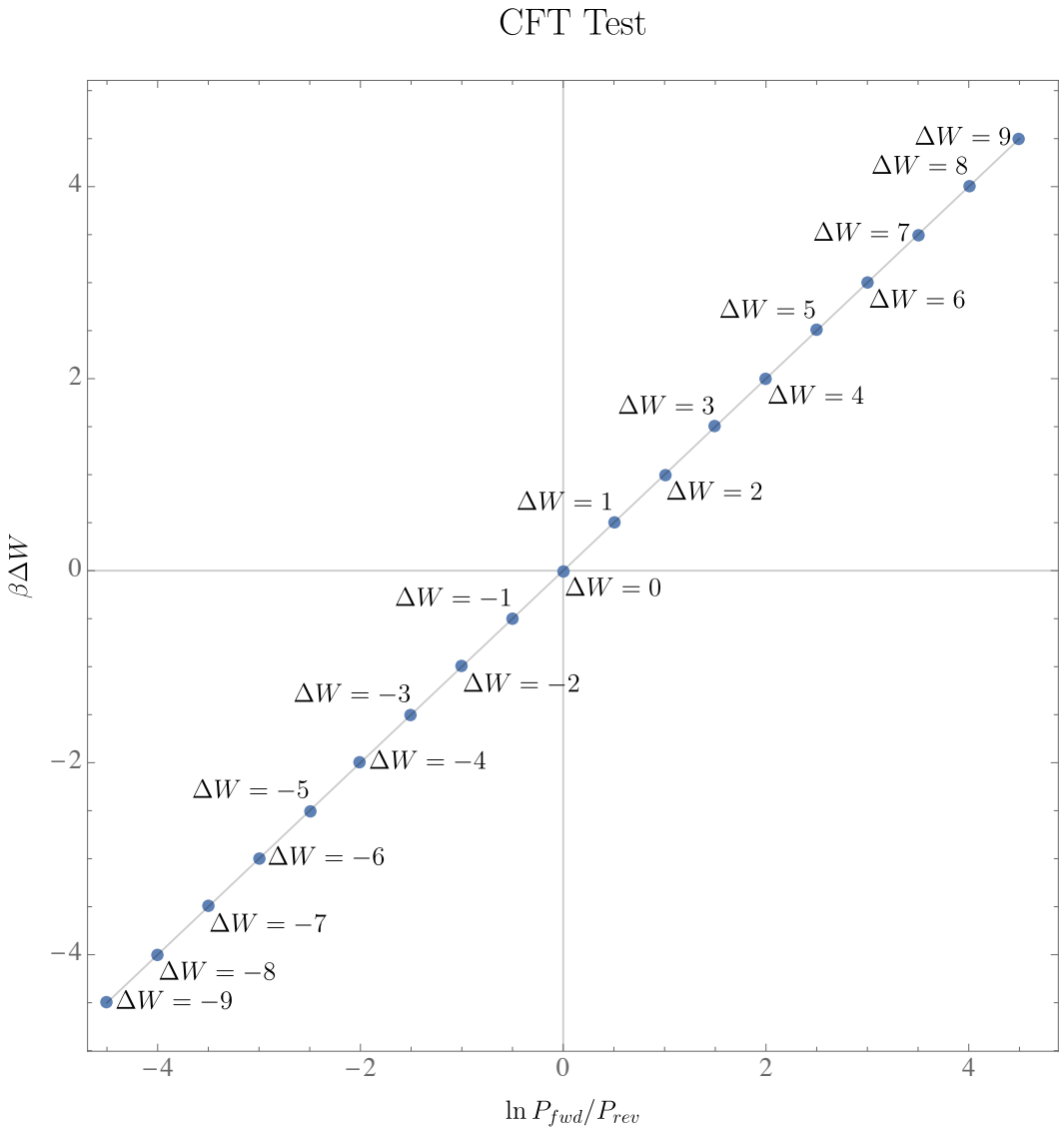

Figure 4.4: Result of the Crooks fluctuation theorem test on the same system as Fig. 4.3. A line of $x = y$ is shown to exemplify how well the points fit the expected values.

Chapter 5

Results and Analysis

In this section, the results from various simulations will be analysed to gain as much physical insight as possible. There are three important energy scales that can be manipulated in these simulations if we consider only hamiltonians which maintain constant eigenvalues, as must be done in order to calculate the full counting statistics of a state.

5.1 Hamiltonian Form

In this investigation we will limit ourselves to two level systems with a constant energy splitting. A physical realisation might be a spin 1/2 particle in a magnetic field with certain characteristics, which will be defined here. In general, such a system can be described by the Hamiltonian

$$H(t) = -\vec{\mu} \cdot \vec{B} = -\mu\vec{\sigma} \cdot \vec{B} \tag{5.1}$$

which has eigenvalues

$$\pm\mu|\vec{B}|. \tag{5.2}$$

This implies that, assuming that the interaction strength of the spin 1/2 system with the magnetic field is time independent, the magnitude of the magnetic field vector must be constant to maintain constant energy splitting. Such a vector can be represented in spherical coordinates, as a function of arbitrary time dependent functions $\alpha(t)$ and $\beta(t)$:

$$\begin{pmatrix} \sin(\alpha(t))\cos(\beta(t)) \\ \sin(\alpha(t))\sin(\beta(t)) \\ \cos(\alpha(t)) \end{pmatrix}. \tag{5.3}$$

Assuming this representation is in a basis where the initial energy splitting is along the z axis, we should choose $\alpha(t)$ to be an arbitrarily chosen constant. Additionally we can define this function such that there is a linear relationship between it and the initial strength of the field in the z direction by choosing $\alpha(t) = \arccos(s)$ where s is the arbitrary constant we will use to define the magnitude of the magnetic field vector along the z axis. As a consequence, the x and y terms will be proportional to $\sqrt{1-s^2}$ and since the magnetic field should not have an imaginary component (which is necessary to ensure that the Hamiltonian is hermitian) this limits the range of our strength parameter to $-1 \leq s \leq 1$. For ease of calculation we set the two eigenvalues to $1/2$ and $-1/2$, which is achieved by setting $\mu = -1/2$ (sign choice is for convenience). We will also use a linearly time dependent oscillation for the x and y components, by setting $\beta(t) = \omega t$

We then arrive at the final hamiltonian which will be used throughout this analysis, by reinserting $\vec{B}$ into equation 5.1

$$H(t) = \frac{1}{2}\begin{pmatrix} s & e^{-i\omega t}\sqrt{1-s^2} \\ e^{i\omega t}\sqrt{1-s^2} & -s \end{pmatrix}. \tag{5.4}$$

There are three parameters which will affect the dynamics of the system: s which determines the strength of the z component of the electric field, and consequently the strength of the oscillatory part of the hamiltonian, the loss rate Γ_- which was described in Sec. 3.3 as determining the rate of energy loss to the environment, and the inverse temperature β which will affect both the initial state of the system, and the rate at which the system will gain energy from the environment.

Additionally the system will always start in the Gibbs state, as this is required in order to use full counting statistics, and is also a requirement of the Crooks fluctuation theorem. For this Hamiltonian, the Gibbs state is given by

$$\frac{1}{2}\left[I - \begin{pmatrix} s & e^{-i\omega t}\sqrt{1-s^2} \\ e^{i\omega t}\sqrt{1-s^2} & -s \end{pmatrix}\tanh(\beta)\right] \tag{5.5}$$

which will be the mixed state for low β and will tend asymptotically towards $1/2\, I - H(t)$ for higher β values.[1]

[1]Both of these formula were calculated symbolically with Wolfram Mathematica and may be quite tedious to derive by hand but are essentially simple derivations. Code is shown in the appendix B.1.3.

5.2 State Dynamics

5.2.1 Effect of the Hamiltonian

If s is chosen to be close to one, an oscillating effect is achieved, with the occupation probabilities of the eigenstates oscillating in a sinusoidal manner. This effect diminishes as s goes from 1 to -1 as shown in Fig. 5.1. If s becomes equal to either 1 or -1 the Hamiltonian becomes time independent, which is not a situation of particular interest in this investigation. It can also be seen in Fig. 5.1 that as s decreases the oscillations become more rapid, but equivalently the amount of oscillation decreases. We will primarily be concerned with situations in which there is greater oscillation of occupancy probability, as this gives rise to more interesting dynamics.

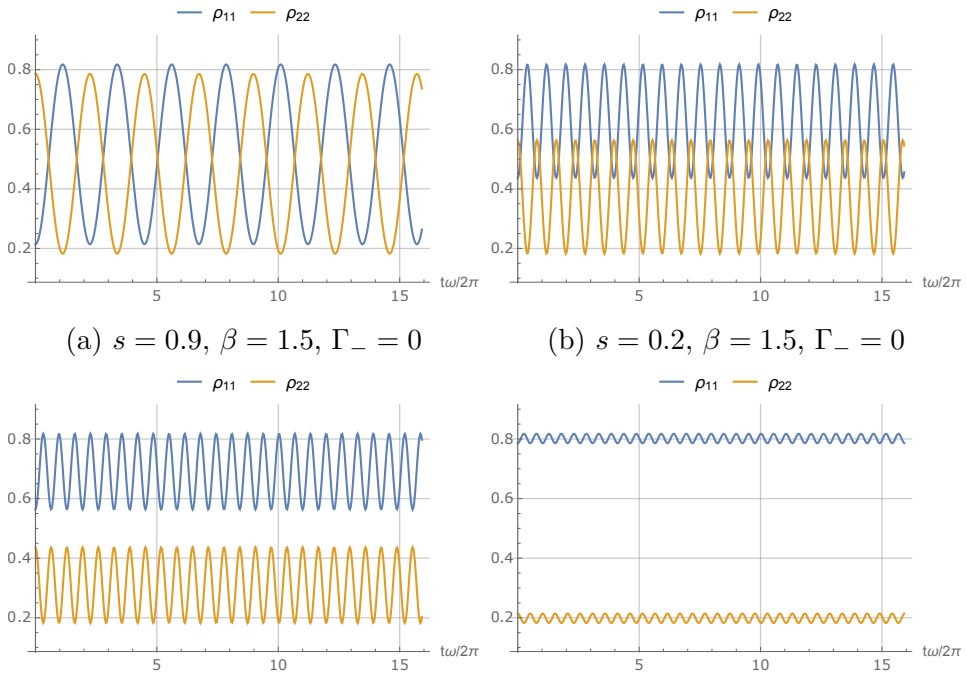

(a) $s = 0.9$, $\beta = 1.5$, $\Gamma_- = 0$ (b) $s = 0.2$, $\beta = 1.5$, $\Gamma_- = 0$

(c) $s = -0.2$, $\beta = 1.5$, $\Gamma_- = 0$ (d) $s = -0.9$, $\beta = 1.5$, $\Gamma_- = 0$

Figure 5.1: Plots showing the occupation probabilities for the two state system undergoing unitary evolution.

5.2.2 The Effect of Temperature

The temperature acts as an overall scale for the system, not only by determining the initial state, but by determining how much energy the system can absorb from the environment relative to the loss rate. At low temperatures the system will tend more slowly to its equilibrium state, but will also start in a more mixed state. The range of inverse temperatures to test can be limited by noting that there is a Tanh relationship to the initial state. Over a certain value (approximately $\beta = 2$) the difference in initial state is inconsequential and the dynamics are very similar.

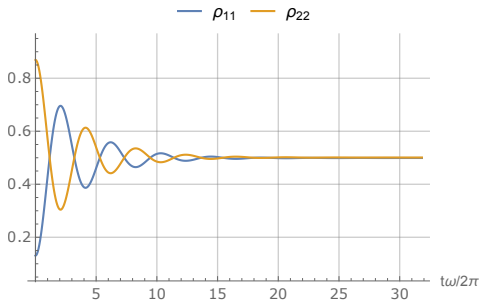

(a) $s = 0.97$, $\beta = 2$, $\Gamma_- = 0.02$

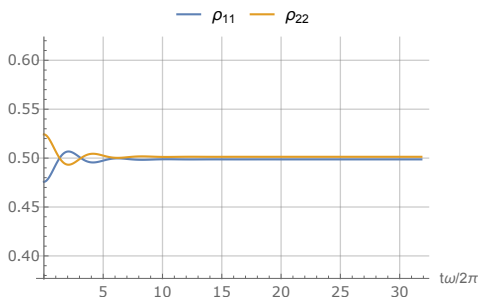

(b) $s = 0.97$, $\beta = 0.1$, $\Gamma_- = 0.02$

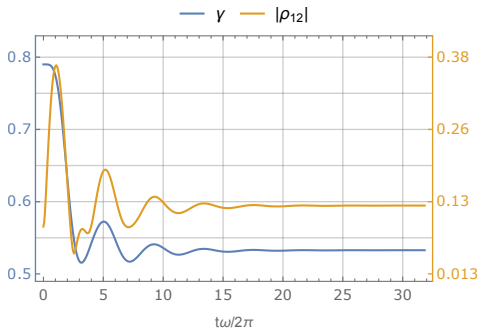

(a) $s = 0.97$, $\beta = 2$, $\Gamma_- = 0.02$

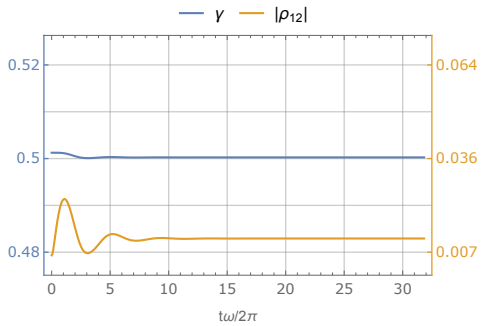

(b) $s = 0.97$, $\beta = 0.1$, $\Gamma_- = 0.02$

Figure 5.3: Plots (a) and (b) show the upper and lower diagonal elements of the density matrix. (c) and (d) show the purity γ and the absolute value of the upper diagonal element of the density matrix, representing the coherence.

We can see from Fig. 5.3 that at lower temperatures the system starts in a state closer in purity to the completely mixed state, and decays more quickly towards it. Additionally it can also be seen that when coming into equilibrium with the environment, the state at a lower temperature has greater purity than the one at a higher temperature, even though the occupation levels decay to approximately the same values. This indicates that the coherence of the state is less affected by the same losses in energy, when the temperature is lower. This is due to the environment exchanging less heat with the system at higher temperatures relative to the amount of work being done on the system, as can be seen in Fig. 5.4.

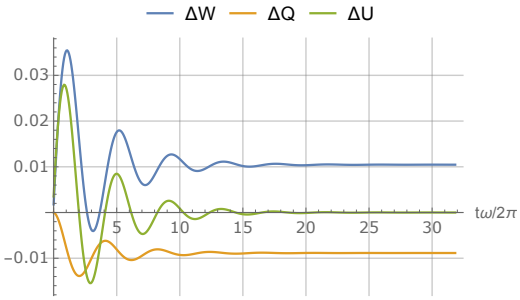

(a) $s = 0.97$, $\beta = 2$, $\Gamma_- = 0.02$

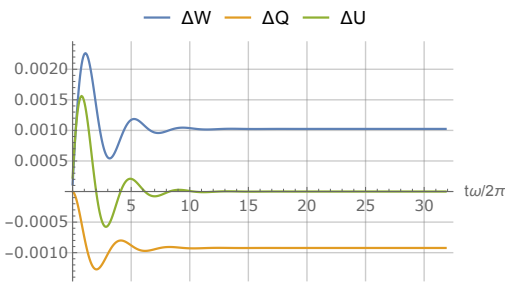

(b) $s = 0.97$, $\beta = 0.1$, $\Gamma_- = 0.02$

Figure 5.4: These plots show the amount of work ΔW and heat ΔQ exchanged with the environment per time step, Additionally the change in the expectation value of the energy of the system ΔU is also shown.

Fig. 5.4 also shows that the amount of heat and work exchanged is lower for higher temperatures. Since the major difference between these two systems is the initial and equilibrium states, we can assert that effect this is due to the system starting in a state closer to the equilibrium state of the driven system, and hence less energy is needed to equilibriate.

5.2.3 The Effect of Loss Rate

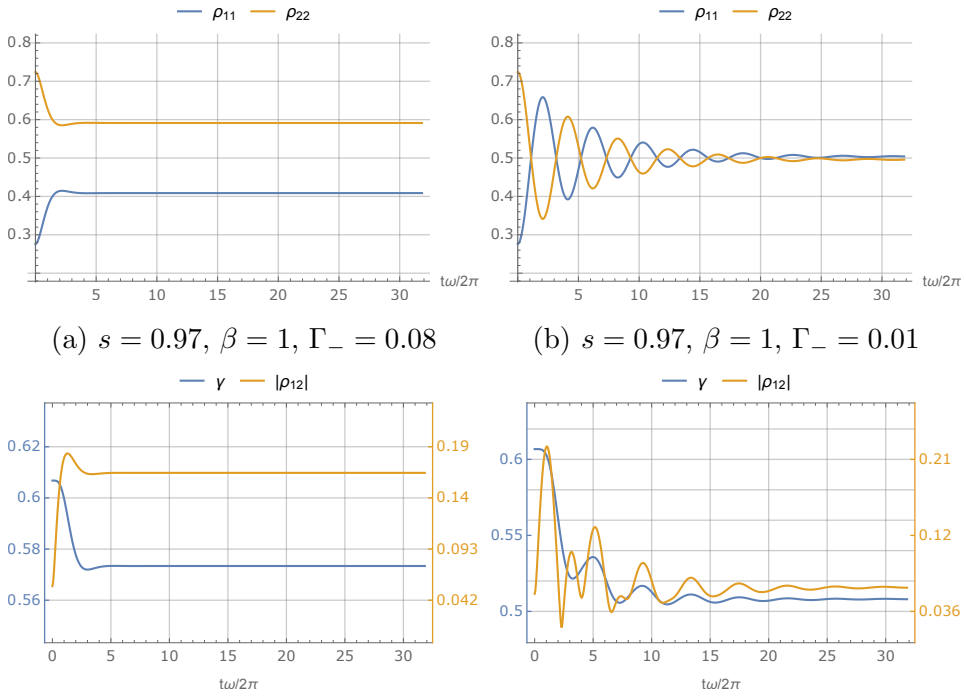

(a) $s = 0.97$, $\beta = 1$, $\Gamma_- = 0.08$ (b) $s = 0.97$, $\beta = 1$, $\Gamma_- = 0.01$

(c) $s = 0.97$, $\beta = 1$, $\Gamma_- = 0.08$ (d) $s = 0.97$, $\beta = 1$, $\Gamma_- = 0.01$

Figure 5.5: Same parameters as Figure 5.3.

If we now consider the effect of loss rate on the system, for a fixed temperature, in-between the two temperature values investigated previously, we find that for higher loss rates the system comes into equilibrium with the driving force over fewer cycles of the oscillation, as can be seen in Fig. 5.5. However, the equilibrium state reached is very different in the two cases. A higher loss rate means that the system is exchanging energy with the environment more rapidly for a given temperature. This means that not only is an equilibrium reached more quickly, but unlike the case of higher temperatures, the eventual equilibrium state still has a relatively high purity, and even has a higher purity then the state with a lower loss rate. This is unexpected as more interaction with an environment, is usually assumed to imply a greater loss of purity for the state. It could be asked whether there is some interaction with the environment that is not described by this model which would negate this effect, but the model represents and random fluctuations of occupancy that fulfils both the detailed balance relation and are Markovian. This is still a very general model of decoherence and there should not be any further physical restrictions that must be imposed on the model, so there should be some physical situation that corresponds to this model (see [5]).

Fig. 5.6 shows that for a higher loss rate, there is a much higher amount of heat exchange with the system. The work and heat exchanges are also approximately equal

at equilibrium which indicates that for higher loss rates, the work being done on the system is balanced by the heat loss to the environment. We can see that the state is still time dependent in Fig 5.7, indicating where the work is going. The Bloch vector is still rotating, but it is not moving in the z axis. Since the detailed balance relation determines the ratio between gain and loss rate, we can assume it is this relation that determines the eventual driven equilibrium of the state for a given hamiltonian.

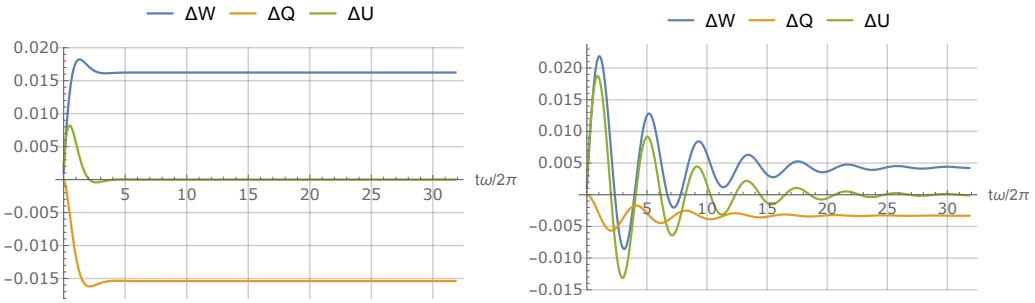

(a) $s = 0.97$, $\beta = 1$, $\Gamma_- = 0.08$ (b) $s = 0.97$, $\beta = 1$, $\Gamma_- = 0.01$

Figure 5.6: Same parameters as Fig. 5.4

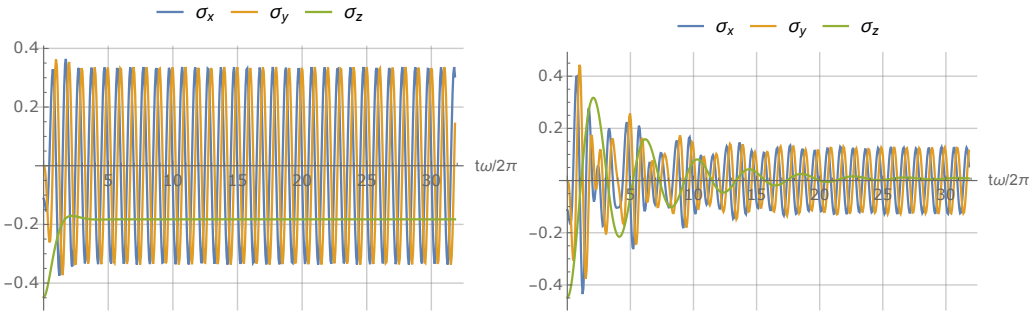

(a) $s = 0.97$, $\beta = 1$, $\Gamma_- = 0.08$ (b) $s = 0.97$, $\beta = 1$, $\Gamma_- = 0.01$

Figure 5.7: These plots show the Bloch components of the state

5.2.4 Effect of Loss Rate and Temperature on State Purity

We now investigate the parameter space of temperature and loss rate, for a given strength parameter, as shown in Fig. 5.8. From this we can interpret several things. First that higher s is, the more susceptible the system will be to loss of purity for low loss rates, and low temperatures. This can be attributed to the fact that low s values (close to -1) The Hamiltonian does very little to change the state, as such equilibrating with the Hamiltonian does not represent a great change from the Gibbs state. As s gets larger, more is done to affect the state and as such driven equilibriums further from the Gibbs state are reached.

Secondly, the lower the temperature, the greater difference there is between the Gibbs state, and the final equilibrium state for the same loss rate as explained in 5.2.2. Finally we can see that higher loss rates at the same temperature result in less difference between the initial and equilibrium states. This is more difficult to explain, however it would appear that the greater the loss rate, the more rapidly the system comes into equilibrium with the driving force, leaving it in a state further away in purity from the completely

mixed state it would have reached eventually if the loss rate was very low (but still greater than zero which is equivalent to unitary evolution).

This last feature might mean that perhaps channels with different loss rates might be used in order to select a particular mixed state with coherences from a nearly pure state without such properties, and store that state without having to completely isolate it from its environment. However, the state will still be decoherent, and it may be unlikely to be of much use in a quantum computing scenario, in which pure states are the ideal. Additionally since the purity will never be higher than that of the original Gibbs state, the storage of such states would only be useful if the state to be stored was different from the Gibbs state of the system, otherwise the operation would be trivial.

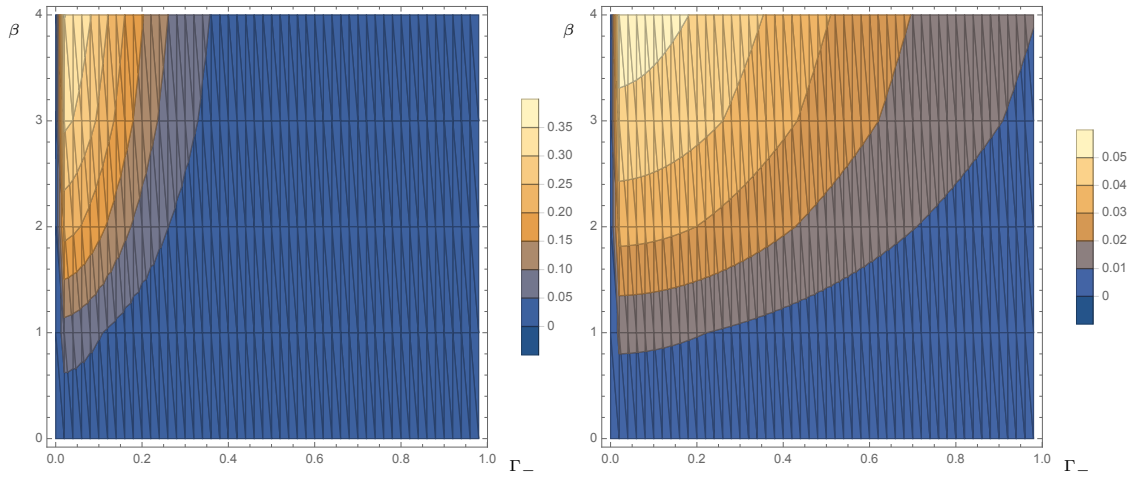

(a) $s = 0.86$

(b) $s = 0$

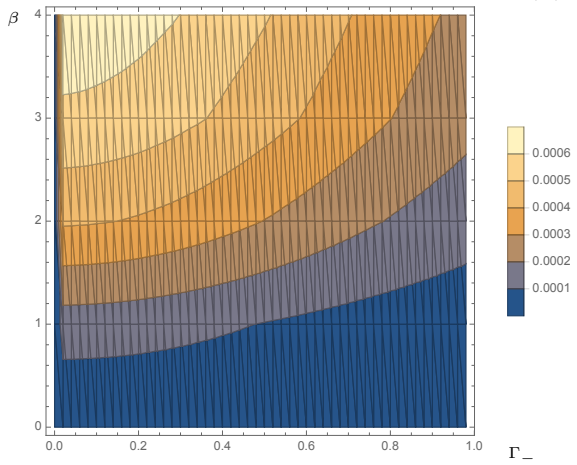

(c) $s = -0.86$

Figure 5.8: Regions correspond to different values for the loss in purity, between a minimum of zero, and maximum of one half. System was sampled at $\beta = 1$ and $\Gamma_- = 0.02$ spaced intervals, and over a time range of $\omega t = 200$, assumed to be enough for the system to reach an equilibrium state. At zero loss rate, there is no difference in purity, as no interaction with the enviroment occurs.

5.2.5 Full Counting Statistics

Through the use of Full Counting Statistics it was possible for the simulation to calculate the probabilities that a an amount of energy equal to a multiple of the level spacing of the system, was either applied to the system as work, or dissipated into the environment through heat, over the entire duration of the evolution of the system. An example is given in Fig. 5.9 which displays the thermal distributions calculated for the system $s = 0.97$, $\beta = 1$, $\Gamma_- = 0.01$. Fig. 5.9 shows each exchange probability as a function of time. The actual number of calculated exchange probabilities is much larger than this, but most are very close to zero.

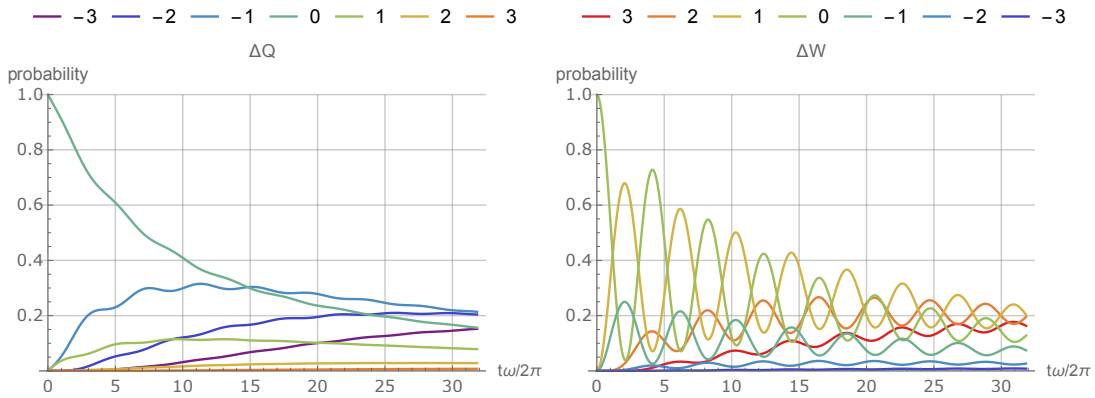

(a) Work and heat Distributions for $s = 0.97$, $\beta = 1$, $\Gamma_- = 0.01$.

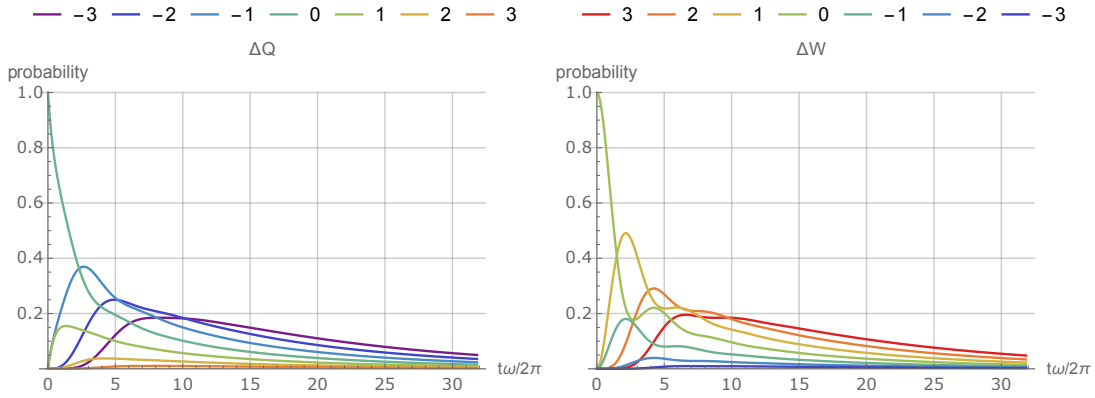

(b) Work and heat Distributions for $s = 0.97$, $\beta = 1$, $\Gamma_- = 0.08$

Figure 5.9: The colours indicate amount of exchange, in accordance with legend shown

From Fig. 5.9 we can see that although the average of heat exchange is negative, and the average of work is positive, there is some small probability to have negative or positive values respectively. This can tell us more about the effect mentioned in Sec. 5.2 in which lower loss rates lead to more mixed equilibrium states. We can see that for the case of higher loss rate, the distributions spread out and drift in the positive and negative direction for work and heat respectively. The drift is due to the fact that the energy exchange probability being calculated is the total energy exchange of the system up to a particular point in time, and since work and heat is constantly exchanged with the system, the average amounts of heat and work exchanged over the entire time of the interaction will grow. The most clear difference between these two situations is that the distribution of energy exchange spreads out more rapidly for higher loss rates. This can

be seen as the probability for energy exchange with the system becoming more random, but also less likely for any specific amount of energy exchange. This means that even though the averages for work and heat exchange are constant, the amount of heat and work exchanged is not.

This can also be investigated by looking at the variance of work and heat, which is calculated here via the characteristic function. In particular the effects of temperature and loss rate are easier to determine when using this method. However, there is a much higher sensitivity to the resolution of the full counting parameter when calculating these quantities, since it depends on derivatives of the function. As such, a higher resolution in the full counting parameter is necessary for accurate results. Fig. 5.10 Shows the change in the second moment, equivalent to the variance, over the evolution of the system.

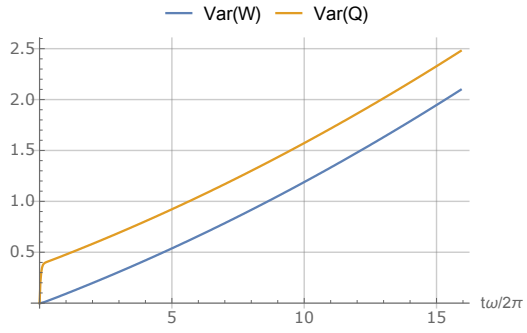

(a) $s = 0.97$, $\beta = 1$, $\Gamma_- = 1$

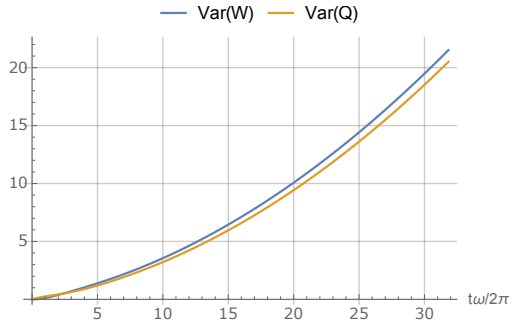

(b) $s = 0.97$, $\beta = 1$, $\Gamma_- = 0.08$

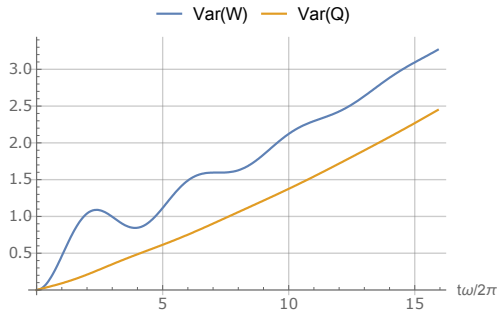

(c) $s = 0.97$, $\beta = 1$, $\Gamma_- = 0.01$

Figure 5.10: These plots show the change in the variance of work and heat over the evolution of the system

We can see clearly from Fig. 5.10 that the variance grows initially much more rapidly for the highest loss rate. Although this growth does not continue for later times, as can be seen in Fig 5.10a. In fact at this high loss rate, the growth of the variance is similar to that of the low loss rate. However, there is a very steep change at the beginning of the time evolution, and the variance in heat is larger than that of the work, unlike the low loss rate situation. If we sample a much smaller time region around this moment, we can see that the heat jumps rapidly to a constant amount of exchange, as does the work, indicating the system jumps within half a cycle of the oscillation to its equilibrium value.

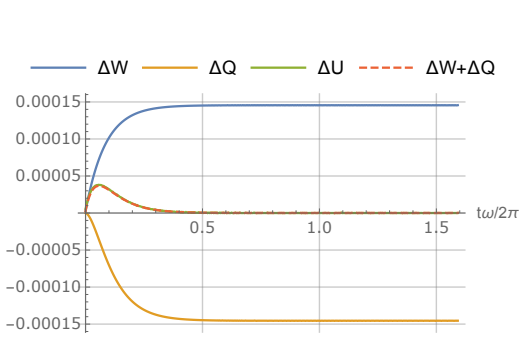

(a) Exchange of heat and work per time step

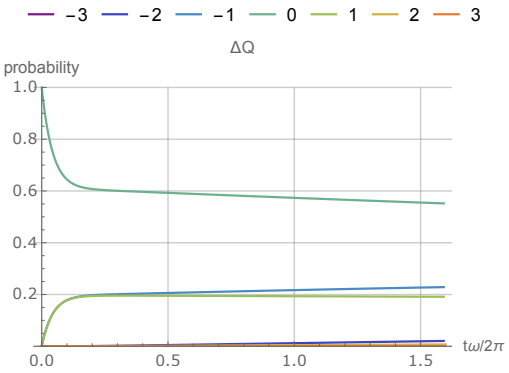

(b) probability distribution for heat

Figure 5.11: $s = 0.97$, $\beta = 1$, $\Gamma_- = 1$ Plots showing the system jumping rapidly into its equilibrium state

Comparing this case to the earlier situation of low loss rates (see Fig. 5.6), we can see that not only is an equilibrium state reached more quickly, but much less energy is exchanged with the system on average. Fig 5.2.5 shows a comparison in the probability distribution for a fixed time

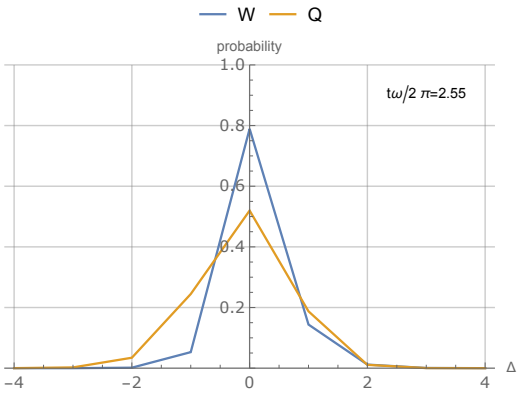

(a) $\Gamma_- = 1$

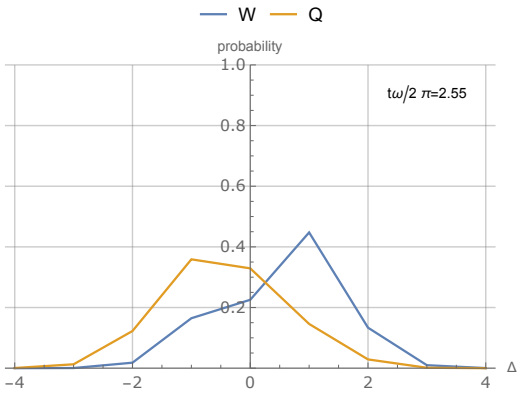

(b) $\Gamma_- = 0.1$

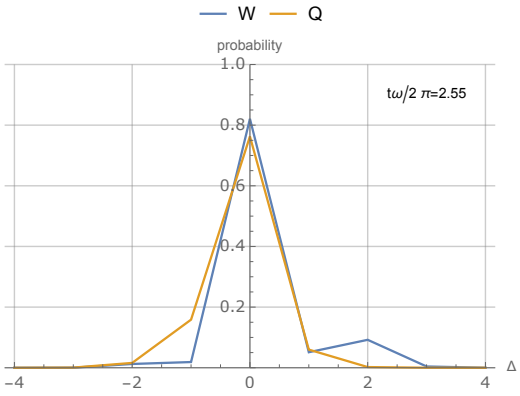

(c) $\Gamma_- = 0.01$

Figure 5.12: $s = 0.92$, $\beta = 1$, Comparison between distributions for $\Gamma_- = 1$, $\Gamma_- = 0.1$ and $\Gamma_- = 0.01$ at $t\omega/2\pi = 8/\pi$

We can see that for the very high loss rate, the distribution stays centred around zero, with some slight skew, giving rise to the average values being close to zero. We can also

see that the heat distribution is wider than the work distribution, indicating that the heat exchange with the system is more random, which is likely due to the greater interaction with the enviroment. For the middle value, the probabilities are more distributed, but have different averages, indicating they have drifted further and that there is a greater average exchange of energy with the environment. The lowest loss rate however, is centred at zero, and has a similar distribution to that of the high loss rate, except with less randomness in the heat exchange.

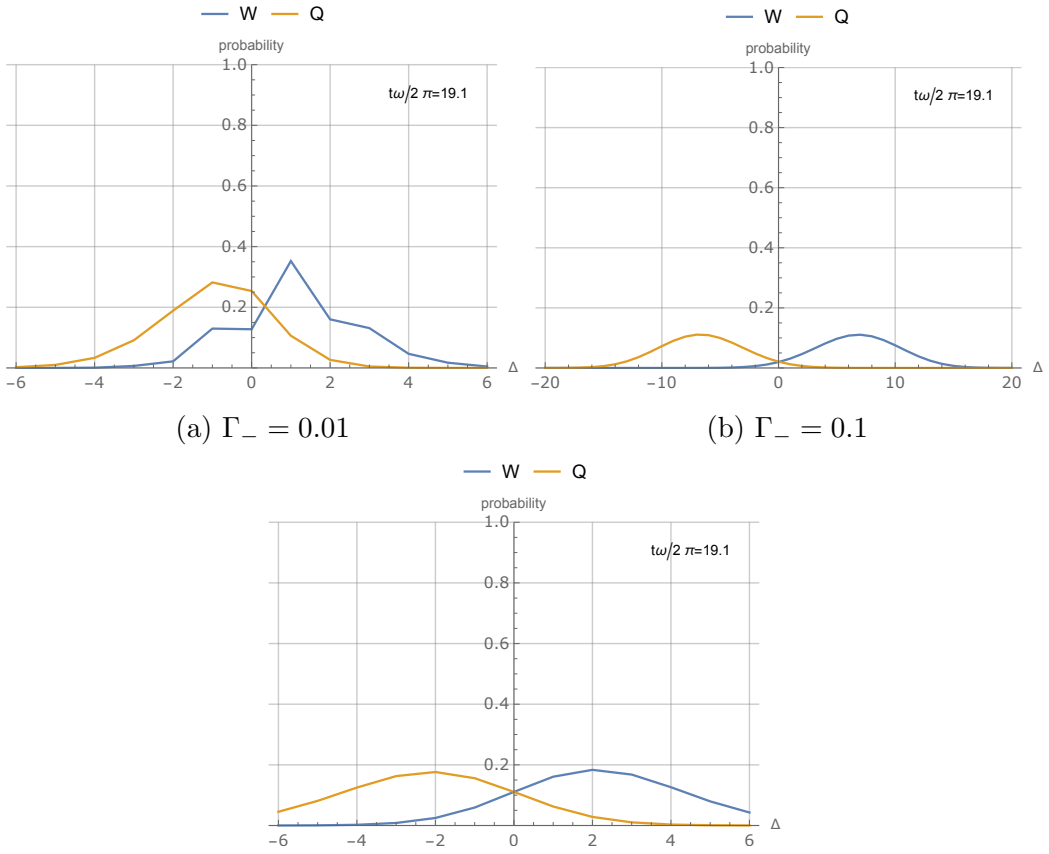

(a) $\Gamma_- = 0.01$ (b) $\Gamma_- = 0.1$

(c) $\Gamma_- = 1$

Figure 5.13: $s = 0.92$, $\beta = 1$ Comparison between distributions for $\Gamma_- = 1$ and $\Gamma_- = 0.01$ at $t\omega/2\pi = 60/\pi$

However Fig. 5.13 shows that at later times, the distributions for $\Gamma_- = 1$ are smoother than for $\Gamma_- = 0.01$ indicating that the system has reached equilibrium, whereas for $\Gamma_- = 0.01$ the system is still exchanging amounts of heat and work that are not evenly distributed and has not yet reached equilibrium. If we then look at the system for $\Gamma_- = 0.1$ We can see that it has interacted with the environment the most. The amount of work and heat exchange is higher than for the other two cases, and the distributions are even more spread out than for the extremely high loss rate. From this we may conclude that as the loss rate increases, there is some value for which interaction with the environment is at its maximum, which can be determined by considering the rate at which the variance of the work and heat distributions increases.

Chapter 6

Outlook

6.1 Summary

This method of simulating qubits in open quantum systems has been able to reveal many properties of the thermal interactions properties of qubits. The simulation was also shown to be in agreement with various well accepted theories, such as the Crooks fluctuation theorem, and the quantum extension of the first law of thermodynamics.

The full counting statistics method was shown to be a useful way of determining the exact distribution of heat and work, and how this information can be used to understand the dynamics of an open quantum system.

We have also gained more insight into the parameters determining the lindblad equation and how they affect the system in question. We have established that there is no simple linear relationship between them, and that the equilibrium state of the driven system is not necessarily the completely mixed state. We determined that this can be analysed by investigating the variance of the system over time.

However the analysis of what the eventual equilibrium state is, was not completed, and will be discussed further in Sec. 6.2

6.2 Extensions

In this section we will discuss possible extensions to the project. Most notably, the analysis of what the eventual equilibrium state is would require more parameter space computations, similar to Fig. 5.8. However to perform these kind of calculations with accurate full counting statistics, takes a long amount of computing time, too much to do rapidly on a home computer (the simulation displayed in this thesis took half a day to complete on a laptop). Running these parameter space calculations on a High performance computer would allow for more detailed scans to be acquired in reasonable amounts of time.

Multiple qubit systems would also be interesting to analyse, as they are very important in quantum computing. This could be achieved with the same theoretical model, however care would have to be taken to ensure that the eigenvalues of the hamiltonian stay constant. Additionally when the full counting statistics is calculated, the discrete Fourier transform must be made over a periodic region. Since the periodicity in the characteristic function will be dependent on the level spacing, care must be taken to ensure that the level spacing allows for a periodicity, which is easily calculable (i.e some small integer ratio).

Appendix A

Open Quantum Systems

A.1 Quantum Thermodynamics

A.1.1 First Law Heat Relation

Using the Liouville-von Neumann equation, we can derive a constant value for $\mathrm{Tr}\, H\partial\rho/\partial t$ under unitary evolution:

$$\begin{aligned}\mathrm{Tr}\left(H\frac{\partial\rho}{\partial t}\right) &= -i\,\mathrm{Tr}\left(H[H,\rho]\right)\\ &= -i\,\mathrm{Tr}\left(HH\rho - H\rho H\right)\\ &= -i(\mathrm{Tr}\left(HH\rho\right) - \mathrm{Tr}\left(H\rho H\right))\\ &= -i(\mathrm{Tr}\left(H\rho H\right) - \mathrm{Tr}\left(H\rho H\right)) = 0\end{aligned} \tag{A.1}$$

Appendix B

Results and Analysis

B.1 Simulation Analysis

B.1.1 Hamiltonian used in Fig. 4.3

$$\begin{pmatrix} \sqrt{5}/6 & (\cos(t) - i\sin(t))/10 \\ (\cos(t) + i\sin(t))/10 & -\sqrt{5}/6 \end{pmatrix} \tag{B.1}$$

B.1.2 Unitary Evolution

```
In[754]:= H[t_] := Cos[t] * PauliMatrix[1] + Sin[t] * PauliMatrix[2]
          ψ[t_] = {up[t], down[t]};
          sys = {ψ'[t] == -I H[t].ψ[t], ψ[0] == {1, 0}};
          sol = DSolve[sys, {up, down}, t];
          ψ[t_] = Simplify[Flatten[ψ[t] /. sol], t ∈ Reals]
```

Figure B.1: Example code for analytic solution to Schrödinger equation, example hamiltonian used is $\cos(t)\sigma_x + \sin(t)\sigma_y$ with initial state $|1\rangle$

B.1.3 Hamiltonian Form

```
In[30]:= μ = -(1 / 2);
         B = {Sqrt[1 - s^2] Cos[ω t], Sqrt[1 - s^2] Sin[ω t], s};
         (H = -μ TrigToExp[Sum[PauliMatrix[i] * B[[i]], {i, 1, 3}]]) // MatrixForm
         FullSimplify[ExpToTrig[MatrixExp[-β H] / Tr[MatrixExp[-β H]]]] // MatrixForm
```

Figure B.2: Code used to symbolically simplify expressions for hamiltonian and Gibbs state expressions

Bibliography

[1] C. H. Bennett and D. P. DiVincenzo, "Quantum information and computation," *Nature*, vol. 404, no. 6775, pp. 247–255, 2000.

[2] C. Pomerance and C. Pomerance, "A tale of two sieves," *NOTICES AMER. MATH. SOC*, vol. 43, pp. 1473–1485, 1996.

[3] P. W. Shor, "Polynomial-time algorithms for prime factorization and discrete logarithms on a quantum computer,"

[4] M. A. Nielsen and I. L. Chuang, *Quantum Computation and Quantum Information: 10th Anniversary Edition*. New York, NY, USA: Cambridge University Press, 10th ed., 2011.

[5] J. H. Buß", "Optical manipulation of a multilevel nuclear spin in zno: Master equation and experiment," *Physical Review B*, vol. 93, no. 15, 2016.

[6] J. Sakurai and J. Napolitano, *Modern Quantum Mechanics*. Addison-Wesley, 2011.

[7] H. P. Breuer and F. Petruccione, *The theory of open quantum systems*. Great Clarendon Street: Oxford University Press, 2002.

[8] P. Cappellaro, "22.51 quantum theory of radiation interactions," 2012.

[9] R. Balian, *From microphysics to macrophysics: methods and applications of statistical physics, Volume I*. Texts and monographs in physics, Springer-Verlag, 1991.

[10] J. Gibbs, *Elementary Principles in Statistical Mechanics: Developed with Especial Reference to the Rational Foundations of Thermodynamics*. Elementary Principles in Statistical Mechanics: Developed with Especial Reference to the Rational Foundation of Thermodynamics, C. Scribner's sons, 1902.

[11] G. E. Crooks, "Entropy production fluctuation theorem and the nonequilibrium work relation for free energy differences," *Phys. Rev. E*, vol. 60, pp. 2721–2726, Sep 1999.

[12] M. Silaev", "Lindblad-equation approach for the full counting statistics of work and heat in driven quantum systems," *Physical Review E*, vol. 90, no. 2, 2014.

[13] P. Talkner, E. Lutz, and P. Hänggi, "Fluctuation theorems: Work is not an observable," *Phys. Rev. E*, vol. 75, p. 050102, May 2007.

[14] M. Am-Shallem, A. Levy, I. Schaefer, and R. Kosloff, "Three approaches for representing lindblad dynamics by a matrix-vector notation," *arXiv preprint arXiv:1510.08634 [quant-ph]*, 10 2015.